Received: 31 December 2019 | Revised: 6 May 2020 | Accepted: 28 May 2020

DOI: 10.1111/cas.14511

ORIGINAL ARTICLE

Cancer Science WILEY

Circular RNA LPAR3 sponges microRNA-198 to facilitate esophageal cancer migration, invasion, and metastasis

Yijun Shi[1] | Na Fang[2] | Yadong Li[1] | Zizhang Guo[1] | Wei Jiang[1] | Yaozhou He[1] | Zijian Ma[1] | Yijiang Chen[1]

[1]Department of Thoracic and Cardiovascular Surgery, The First Affiliated Hospital of Nanjing Medical University, Nanjing, China

[2]Department of Molecular Cell Biology and Toxicology, Center for Global Health, School of Public Health, Nanjing Medical University, Nanjing, China

Correspondence
Yijiang Chen, Department of Thoracic and Cardiovascular Surgery, The First Affiliated Hospital of Nanjing Medical University, Nanjing, China.
Email: chenyjnjmu@163.com

Funding information
National Natural Science Foundation of China, Grant/Award Number: 81572263

Abstract

In this study, we explored expression and functions of circular RNA LPAR3 (circLPAR3) in esophageal squamous cell carcinoma (ESCC). The differential expression of circular RNAs (circRNAs) in 10 ESCC and corresponding paracarcinoma tissues was analyzed through circRNA microarray, then the candidate circRNAs were detected and verified through quantitative RT-PCR, and a novel circRNA was screened, which was circLPAR3. Circular RNA LPAR3 showed apparently high expression in ESCC tissues and cells, which was closely correlated with the clinical stage and lymph node metastasis of ESCC patients. Circular RNA LPAR3 was mainly located in the cytoplasm of ESCC cells, which was more stable than the baseline gene. Circular RNA LPAR3 upregulated *MET* gene expression through sponge adsorption of microRNA (miR)-198, activated the RAS/MAPK and the PI3K/Akt pathways, and promoted ESCC cell migration, invasion, and metastasis in vivo and in vitro. However, it had no effect on ESCC cell proliferation. Circular RNA LPAR3 can regulate the miR-198-MET signal axis to promote the migration, invasion, and metastasis of esophageal cancer cells, which can thereby serve as a potential diagnostic and therapeutic target of esophageal cancer.

KEYWORDS

circLPAR3, circular RNA, esophageal squamous cell carcinoma, MET, miR-198

1 | INTRODUCTION

Esophageal cancer is one of the common digestive tract malignant tumors, which has severely threatened human health. Esophageal cancer ranks 6th among the causes of cancer-related death worldwide,[1] and its 5-year overall survival is only 20%-40%.[2] With the development of early diagnosis, radical operation, and postoperative adjuvant therapy in recent years, the prognosis for EC patients is partially improved, and the 5-year survival rate for early EC is as high as 86%.[3] The high mortality rate of EC is related to distant organ recurrence and metastasis progression. Therefore, it is urgent to investigate EC and its metastatic pathogenesis at the molecular level, and to propose the prediction and intervention strategies for EC and its metastasis.

Esophageal cancer can be mainly divided into 2 major pathological types, esophageal squamous cell carcinoma (ESCC) and

Yijun Shi and Na Fang contributed equally to this work.

esophageal adenocarcinoma (EAC); ESCC accounts for up to 80% of cases.[4]

Circular RNAs (circRNAs) are a class of novel endogenous noncoding RNAs, which can regulate gene expression in eukaryotes. Circular RNAs can form a closed circular molecule that is free of linear RNA 5′- and 3′-terminal by means of reverse splicing.[5,6] Such circular molecules are not susceptible to the RNA exonuclease, which thereby have a more stable structure than linear RNA.[7] There are diverse circRNAs in mammalian cells, which are conserved.[8-10] Generally, they can specifically express at the tissue development period, and exert vital roles in numerous physiological and pathological processes,[11,12] including microRNA (miRNA) sponge, regulation of gene transcription, RNA binding protein, and protein translation. The exonic circRNA can serve as the sponge to adsorb miRNAs, so as to finely regulate miRNA-mediated gene expression.[13-15] Increasing studies have verified that circRNAs play key roles as tumor suppressor genes or oncogenes in the genesis and development of various cancers, including EC proliferation and progression.[16] Nonetheless, the circRNA expression profiles, function and regulation in ECs remain to be further investigated.

In this study, the differential expression of circRNAs in 10 EC tissues and paracarcinoma tissues was analyzed through circRNA microarray; in addition, the screened circRNAs were further verified in EC tissues using the quantitative RT-PCR (qRT-PCR) technique, so as to identify the novel circRNA, circLPAR3. Circular RNA LPAR3 showed apparently high expression in EC tissues and cells; in addition, circLPAR3 expression in EC tissues was positively correlated with clinical stage and lymph node metastasis (LNM). In in vitro experiments, circLPAR3 promoted EC cell migration and invasion, and it enhanced the lung metastasis of EC cells in in vivo experiments. Mechanically, circLPAR3 served as the sponge to adsorb miR-198 and upregulate MET, so as to form the circLPAR3-miR-198-MET signal axis, which further promoted EC cell migration. Consequently, circLPAR3 might be an important factor of EC development and metastasis.

2 | MATERIALS AND METHODS

2.1 | Esophageal squamous cell carcinoma patient samples

The fresh frozen ESCC tissues and corresponding paracarcinoma tissues were derived from 52 patients undergoing radical resection of EC at the Affiliated People's Hospital of Jiangsu University. All patients were naive to radiotherapy or chemotherapy before surgery. All specimens were immediately preserved in liquid nitrogen after surgery. Each patient had complete clinical and pathological data. This study was approved by the Ethics Committee of the Affiliated People's Hospital of Jiangsu University, and all patients had signed the informed consent before the study.

2.2 | Cell culture

The ESCC cell lines ECA109, TE-13, Kyse150, Kyse450, and Kyse510, as well as the normal esophageal epithelial HET-1A cells, were purchased from the Shanghai Cell Bank of the Chinese Academy of Sciences. Afterwards, all cells were cultured in RPMI-1640 culture medium supplemented with 1% streptomycin, 1% penicillin, and 10% FBS, and incubated at 37°C in 5% CO_2 conditions.

2.3 | Circular RNA microarray analysis

Total RNA was extracted from 10 pairs of ESCC samples, and linear RNA was removed through RNase R (Epicenter) digestion. Thereafter, the enriched circRNA was amplified and transcribed into fluorescent cRNAs, followed by analysis using the Arraystar Human circRNA Array (8 × 15K; Arraystar). The microarray was scanned by the Agilent scanner G2505C, the collected images were analyzed through the Agilent feature extraction software (11.0.0.1 version), and the obtained data were analyzed.

2.4 | RNA extraction and quantitative real-time PCR

The intracellular total RNA was extracted using TRIzol reagent (Invitrogen), and the tissue sample total RNA was extracted using the GeneJET RNA Purification Kit (Invitrogen) in accordance with the reagent instructions. The RT SuperMix reverse transcription kit (Vazyme Biotech) was used to reverse transcribe RNA into cDNA, and the SYBR Premix Ex Taq II (Vazyme Biotech) was used for qRT-PCR. The relative gene expression level was calculated according to the $2^{-\Delta\Delta CT}$ method, GAPDH was used to normalize the relative expression levels of circRNA and linear mRNA, whereas U6 was utilized to normalize the miRNA expression level. All primers and the related sequences used in the experiment are listed in Table 1.

TABLE 1 Primer sequences used in this study

Primer name	Sequence (5′-3′)
circLPAR3 For	GAGTTACCTTGTTTTCTGGACA
circLPAR3 Res	TGGAGAAGTGAACATCCTAAG
Met For	CACTTCTGAGAAATTCATCAGGCTGTGAAG
Met Res	ATCTGTCAATCCTGTCCGTGT
18S For	GGAGTATGGTTGCAAAGCTGA
18S Res	TCCTGCTTTGGGGTTCGATT
U6 For	CTCGCTTCGGCAGCACA
U6 Res	AACGCTTCACGAATTTGCGT
GAPDH For	GGGAAGCTCACTGGCATGGCCTTCC
GAPDH Res	CATGTGGGCCATGAGGTCCACCAC
LPAR3 For	GGGTCCATAGCAACCTGACC
LPAR3 Res	GGGAAGAGCAGGCAGAGATG

Abbreviations: For, forward; Res, reverse.

2.5 | Small interfering RNA, miRNA, shRNA, and plasmid construction

The plasmid with high LPAR3 expression, high circLPAR3expression, and the siRNAs targeting circLPAR3 were designed and synthesized by RiboBio (Guangzhou, China). In addition, shRNA targeting circLPAR3 was designed based on the siRNA sequence, which was then cloned into the pGLV3/H1/GFP/Puro vector (GenePharma). MicroRNA-198 mimic, miR-198 inhibitor, and the corresponding control sequences were designed and synthesized by GenePharma. The si-circLPAR3, miR-198 mimic/negative control (NC), and miR-198inhibitor/NC sequences used in experiment were shown in Table 2.

2.6 | Cell Counting Kit-8 assay

Esophageal squamous cell carcinoma cell proliferation was detected according to the CCK-8 assay. In brief, 2000 ESCC cells were inoculated into the 96-well plate, and 10 μL CCK-8 solution was added into each well after 24, 48, 72, and 96 hours of transfection (Dojindo) to culture for 2 hours at 37°C. The absorbance value was measured at the wavelength of 450 nm.

2.7 | Colony formation assay

Five hundred Kyse450 cells were inoculated into each well of 6-well plates and cultured continuously for 14 days. Thereafter, cells were fixed with methanol for 1 hour, and the colonies formed were counted at 1 hour after crystal violet staining.

2.8 | Transwell assays

After 48 hours of cell transfection, 100 μL serum-free culture solution containing 2×10^4 ESCC cells was added into the upper Transwell chamber (8-μm pore size). In the invasion assay, the upper chamber was coated with Matrigel (BD Biosciences), while 600 μL culture solution was added to the lower chamber containing 10% FBS. Later, the TE13 cells were cultured for 12 hours, and the Kyse450 cells were cultured for 24 hours. Cells that penetrated the chamber diaphragm were fixed with methanol for 1 hour and stained with crystal violet (Beyotime Biotechnology) for 30 minutes. All cells were then magnified under a microscope at 200× magnification, and 5 fields of view were randomly selected for observation and counting.

TABLE 2 Circular RNA LPAR3 siRNA (si-circLPAR3), microRNA (miR)-198 mimic/negative control (NC), and miR-198 inhibitor/NC sequences used in this experiment

Name	Sequence (5′-3′)
si-circLPAR3#1	CTAGGTTTGAAAGACTAAT
si-circLPAR3#2	AGGTTTGAAAGACTAATAG
si-circLPAR3#3	TGAAAGACTAATAGGGATG
miR-198 mimic sense	GGUCCAGAGGGGAGAUAGGUUC
miR-198 mimic antisense	ACCUAUCUCCCCUCUGGACCUU
miR-198 mimic-NC sense	UUCUCCGAACGUGUCACGUTT
miR-198 mimic-NC antisense	ACGUGACACGUUCGGAGAATT
miR-198 inhibitor	GAACCUAUCUCCCCUCUGGACC
miR-198 inhibitor-NC	CAGUACUUUUGUGUAGUACAA

2.9 | RNase R treatment assay

Six units of RNase R (Geneseed Biotech) were added into every 2 μg RNA and incubated at 37°C for 20 minutes. After RNase R treatment, the mRNA expression of circLPAR3 and LPAR3 was detected by qRT-PCR.

2.10 | RNA FISH

The cy3-labeled circLPAR3 probe was purchased from RiboBio. Then the probe signal was detected using the FISH kit (RiboBio) according to the manufacturer's instructions. Zeiss AIM software and the Zeiss LSM 700 confocal microscope system (Carl Zeiss) were used to capture the confocal images of cells.

2.11 | RNA nuclear-cytoplasmic separation experiment

The nuclear and cytoplasmic RNA was extracted using the PARIS kit (Invitrogen) in accordance with the manufacturer's instructions. The relative expression quantities of circLPAR3 in the cell nucleus and cytoplasm were detected by qRT-PCR.

2.12 | RNA immunoprecipitation assay

The EZMagna RIP kit (Merck) was utilized to accomplish the RNA immunoprecipitation (RIP) assay. In brief, the RIP lysis buffer was used in ESCC cell lysis, and the lysate was incubated for 6 hours with the magnetic beads previously binding to anti-Argonaute 2 (AGO2) (Abcam) or anti-IgG Ab. Afterwards, the magnetic beads were cleaned and digested with proteinase K to remove the protein. Finally, the purified RNA was analyzed through qRT-PCR.

2.13 | Dual-luciferase reporter gene assay

Circular RNA LPAR3-wt or circ0006168-mut was constructed into the dual-luciferase reporter vector (GP-miRGLO). Kyse450 cells were cultured for 24 hours in a 24-well plate at the density of 5×10^4 cells/well for transfection. Lipofectamine 2000 (Invitrogen) was used to cotransfect the dual-luciferase reporter gene plasmid and miR-198 mimics or miR-198 mimic-NC into Kyse450 cells.

Forty-eight hours later, the luciferase activities were measured using the dual-luciferase reporter detection kit (Promega).

2.14 | Western blot analysis

Cells were cultured for 48 hours after cell transfection, the protein was extracted using the RIPA lysis buffer (Thermo Fisher Scientific), and quantified using the BCA kit (Beyotime Biotechnology). Sample (30 μg) was collected, separated through 10% PAGE, and electronically transferred onto the PVDF membranes. Then the membranes were blocked with blocking solution at 37°C for 1 hour under gentle shaking in the shaking table. Thereafter, primary Abs were added to incubate at 4°C overnight and secondary Ab was added to incubate at 37°C for 1 hour. Chemiluminiscence was detected by the enhanced chemiluminescence system (Yeasen), then processed and analyzed by the gel imaging system. Tubulin was used as the internal reference protein. The experiment was repeated 3 times. The Abs used in this experiment were as follows: MET (1:2000; Abcam); P-Akt (1:2000; Proteintech); P-MAPK (1:2000; Cell Signaling Technology), Tubulin (1:1000; Beyotime Biotechnology), and HRP-conjugated secondary Ab (1:1000; Beyotime Biotechnology).

2.15 | Animal studies

All animal experiments were proved by the Institutional Animal Care and Use Committee of Nanjing Medical University. Each 5-week-old BALB/c nude mouse was injected with 100 μL TE13 cells with stably low circLPAR3#3 expression (shcircLPAR3#3) or control cells (shRNA control) through the caudal vein at the cell density of 1×10^7 cells/mL. Mice were killed at the 6th week after caudal vein injection, the lung tissues were dissected and photographed, the lung tissue pathological sections were used for H&E staining and immunohistochemical (IHC) examination, and the number of lung tumor metastasis was counted.

2.16 | Statistical analysis

The SPSS 22.0 (IBM) statistical analysis software was adopted for data analysis. All experimental data were expressed as mean ± SD. Pairwise comparison between 2 groups was carried out by *t* test, and the correlations of circLPAR3 expression with clinical parameter characteristics were analyzed by Pearson's χ^2 test. A difference of $P < .05$ was deemed as statistically significant.

3 | RESULTS

3.1 | Circular RNA LPAR3 expression level increased in human ESCC tissues and cell lines

To investigate circRNAs expression in EC tissues, the 10 pairs of EC and paracarcinoma tissues were carried out circRNA microarray analysis, and the circRNA expression patterns were displayed through hierarchical clustering between ESCC tissues and paracarcinoma tissues (Figure 1A). Changes in the circRNA expression were discovered in the volcano (Figure 1B) and scatter (Figure 1C) plots. Microarray results suggested that, compared with paracarcinoma tissues, circCNOT6L had the most obvious elevation, followed by circLPAR3; in addition, the top 10 candidate circRNAs in terms of fold upregulation were selected from the detection results for further analysis (Table 3). Subsequently, they were verified in the 10 pairs of ESCC and paracarcinoma tissues through qRT-PCR. As was observed, these 10 candidate circRNAs were upregulated, which was consistent with the microarray results, but circLPAR3 had the highest fold of differential expression (Figure 1D). As a result, *circLPAR3* was selected as the target gene for investigation. Then circLPAR3 was detected in various ESCC cell lines, as well as in the 52 pairs of EC and paracarcinoma tissues through qRT-PCR, and the results suggested that circLPAR3 expression was apparently upregulated in ESCC tissues and cell lines (Figure 1E,F). Expression of circLPAR3 in ESCC tissues was markedly higher than that in paracarcinoma tissues; in addition, the high circLPAR3 expression was correlated with LNM and advanced TNM stage, but not with age, sex, tumor infiltration depth, or tissue differentiation degree (Table 4). These experimental data revealed that circLPAR3 promoted the invasion and metastasis of ESCC.

3.2 | Biological characteristics of circLPAR3 in ESCC

According to the circBase database, circLPAR3 was derived from the linear gene *LPAR3* located on chromosome 1, which was formed through the single cyclization of exon 2 on LPAR3 mRNA and was 754 bases in length (Figure 2A). To investigate its characteristics in ESCC, we had designed the circLPAR3 back-to-back primers for gene amplification and base sequencing, and our results confirmed the presence of a shearpoint sequence of reverse splicing of exon 2 in the circLPAR3 sequence (Figure 2B). Afterwards, total RNA was extracted from the ESCC Kyse450 cells, and the 3′-5′ exoribonuclease-RNase R was added for digestion. The processed RNA was detected through qRT-PCR after reverse transcription, which suggested that the linear LPAR3 mRNA was apparently degraded, but it made no distinct difference to the expression of the closed circular circLPAR3 (Figure 2C). The above results confirmed that circLPAR3 had superior stability in ESCC cells to its linear LPAR3 mRNA. The FISH assay and RNA nuclear-cytoplasmic separation results revealed that circLPAR3 was mainly distributed in the cytoplasm of ESCC cells, while a small portion was located in the nucleus (Figure 2D,E). The above experiments verified that circLPAR3 was an exonic circular RNA that was mainly located in the cytoplasm of ESCC cells.

3.3 | Circular RNA LPAR3 promoted migration and invasion of ESCC cell lines in vitro

Three siRNAs were designed at the reverse connection site formed by circLPAR3, and qRT-PCR detection was carried out after transfection

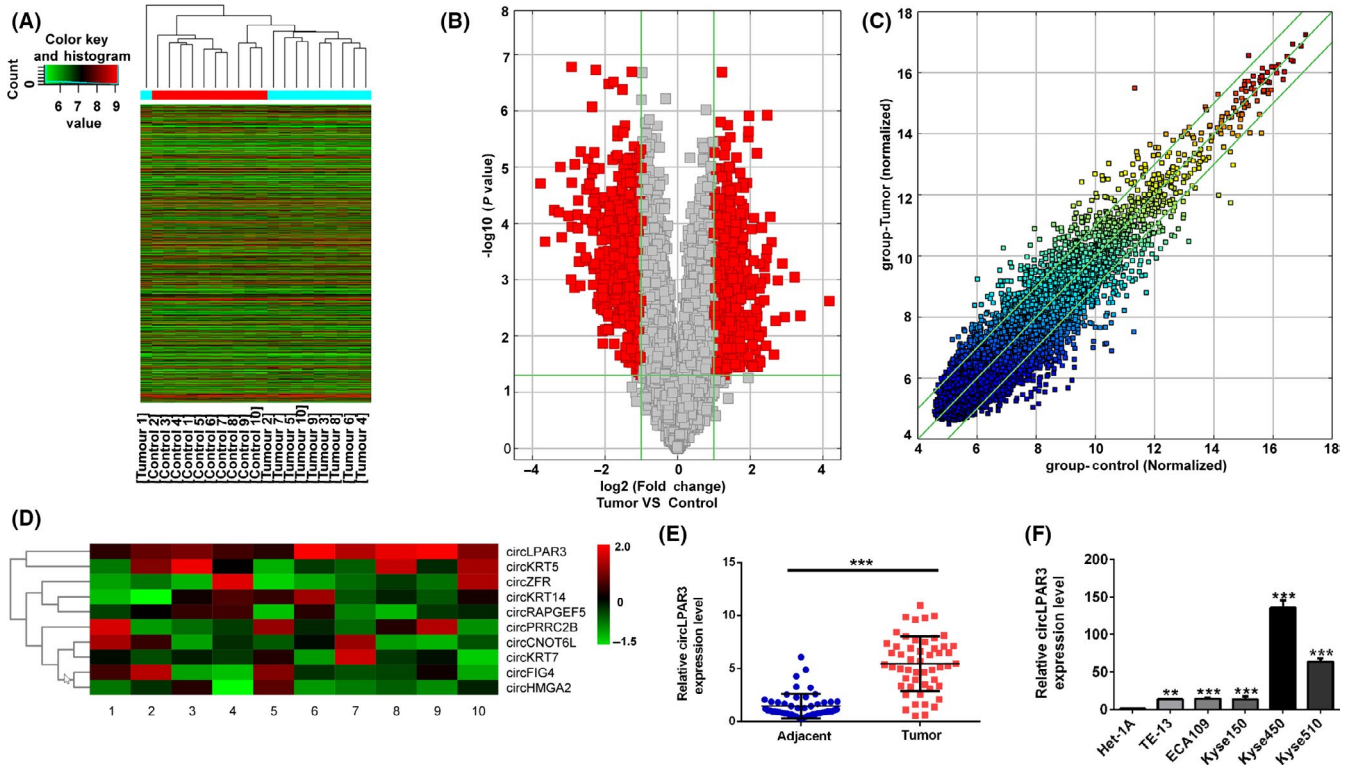

FIGURE 1 Screening of target gene circular RNA LPAR3 (circLPAR3) as the biomarker of esophageal squamous cell carcinoma (ESCC) invasion and metastasis. A, The high-throughput sequencing results of 10 pairs of ESCC and paracarcinoma tissues, the differential expression of circRNA in ESCC and paracarcinoma tissues is analyzed through heat map and hierarchical clustering analysis, and the relative expression levels of circRNA were arranged from the highest to the lowest levels, as denoted in red and green, respectively. B, The *X* axis in the volcano plot represents the fold change (FC); the *Y* axis indicates the *P* value. The *P* value at the green boundary = .05, FC = 2.0, and the red points in the plot represent the differentially expressed circRNAs. C, Scatter plot is drawn to learn the expression data distribution in the microchip, and a greater data scattering degree indicates a greater difference degree. *X* and *Y* axes indicate the signal values after standardization, in which the green line stands for the FC. In this experiment, the differential expression standards are set at FC ≥ 2.0 or ≤0.5, which refer to the region above the upper green line and the region below the lower green line in the plot, respectively. D, CircLPAR3 expression in 10 pairs of ESCC and paracarcinoma tissues verified by qRT-PCR. E, CircLPAR3 expression in 52 pairs of ESCC tissues and matched paracarcinoma tissues detected by quantitative RT-PCR. F, CircLPAR3 expression in ESCC-related cell lines. $^{**}P < .01$, $^{***}P < .001$

TABLE 3 Top 10 upregulated circular RNAs (circRNAs) detected by circRNA microarray sequencing

circRNA	Regulation	FC	*P*-value	Chrom	circRNA type
circCNOT6L	Up	18.1	.002	chr4	Exonic
circLPAR3	Up	10.4	.004	chr1	Exonic
circKRT14	Up	9.3	.000	chr17	Exonic
circKRT7	Up	7.7	.004	chr12	Exonic
circZFR	Up	7.4	.000	chr5	Exonic
circHMGA2	Up	6.8	.001	chr12	Exonic
circKRT5	Up	6.5	.005	chr12	Exonic
circRAPGEF5	Up	6.3	.021	chr7	Exonic
circFIG4	Up	6.0	.000	chr6	Exonic
circPRRC2B	Up	5.8	.000	chr9	Intronic

Abbreviations: Chrom, chromosome; FC, fold change.

of ESCC cells. These 3 siRNAs specifically knocked out circLPAR3 expression, among which, si-circLPAR3#2 and si-circLPAR3#3 had better knockout effect, without affecting the expression of its linear gene *LPAR3* (Figure 3A-C). After circLPAR3 KO in Kyse450 cells, Transwell assay results indicated that the cell migration and invasion capacities were apparently suppressed (Figure 3D). Transfection of high circLPAR3 expression plasmid in Kyse450 cells markedly upregulated the circLPAR3 expression level, but it did not affect the expression level

TABLE 4 Relationship between circular RNA LPAR3 (circLPAR3) expression and clinicopathologic features of esophageal squamous cell carcinoma

Characteristic	All patients	CircLPAR3 low expression	CircLPAR3 high expression	*P* value
N	52	26	26	
Age (y)				
<60	4	1	3	.611
≥60	48	24	24	
Gender				
Male	40	22	18	.188
Female	12	4	8	
Histological grade				
Moderate	38	17	21	.427
Poor	14	8	6	
Tumor infiltration depth				
T1-T2	30	18	12	.092
T3-T4	22	8	14	
TNM stage				
I-II	26	19	7	.001**
III-IV	26	7	19	
Lymph metastasis				
Yes	26	7	19	.001**
No	26	19	7	

**$P < .01$.

of its linear gene *LPAR3* (Figure 3E-G). Transfection of LPAR3 overexpression plasmid into TE-13 cells not only successfully increased the expression of linear LPAR3, but also increased circLPAR3 expression in TE-13 cells (Figure 3H,I). Similarly, the Transwell assay showed that high circLPAR3 expression promoted the migration and invasion capacities of ESCC cells (Figure 3J). Additionally, cell colony formation and CCK-8 assays were carried out to detect the effect of low circLPAR3 expression in Kyse450 cells on cell proliferation, and our results revealed no obvious difference in cell proliferation between low circLPAR3 expression group and control group (Figure 3K,L).

3.4 | Circular RNA LPAR3 served as miRNA sponge for miR-198 in ESCC cells

Our research results suggested that circLPAR3 promoted ESCC cell migration and invasion, but the precise molecular mechanism remains unclear. Using Arraystar's home-made software, it was predicted that 5 miRNAs had the binding sites with circLPAR3, including miR-198, miR-2682-5p, miR-4692, miR-6511a-5p, and miR-6780-5p. Moreover, the seed sequence located in the 5′-terminal of miRNA (No.2-7nt) forms the Watson-Crick pair with target gene 3′UTR, which is the most important factor in the prediction of all miRNA target genes. The specificity efficiency is shown below: 8mer > 7mer-m8 > 7merA1 > 6mer. Typically, the binding site of circLPAR3 with miR-198 belonged to the 8mer site type (Figure 4A), which had higher specificity than other miRNA bindings. Additionally, numerous studies had reported the close relationship of miR-198 with tumor, whereas the association of the remaining 4 miRNAs with tumor had not been reported. Therefore, miR-198 was selected as the preferred object of study. The downstream target gene of miR-198 was predicted based on databases PicTar, miRTarBase, TargetScan, and miRBase, and the intersection of these 4 databases was obtained to acquire a target gene, *MET* (Figure 4B); additionally, the binding site of the circLPAR3-miR-198-MET seed sequence was predicted using TargetScan software (Figure 4C). Based on the binding site of circLPAR3 with miR-198, the circLPAR3 WT and mutant dual-luciferase reporter gene plasmids were designed and synthesized (Figure 4D), and the circLPAR3 WT or mutant plasmids were cotransfected into TE13 cells with miR-198 mimics or miR-198 mimic-NC. The results suggested that, miR-198 only reduced the luciferase activity of circLPAR3 WT plasmid, but it had no influence on the luciferase activity of the circLPAR3 mutant plasmid (Figure 4E). In Kyse450 and TE13 cells, RIP experimental results revealed that, compared with IgG group, miR-198 and circLPAR3 expression levels in the Ago2 group were notably higher than those in the control group (Figure 4F,G). The above experiments verified that circLPAR3 served as a sponge of miR-198 in ESCC cells.

3.5 | Circular RNA LPAR3 targeted *MET* through sponge adsorption of miR-198

Quantitative RT-PCR and western blotting experimental results revealed that overexpression of miR-198 in TE13 cells apparently downregulated MET mRNA and the coded c-MET protein levels, whereas miR-198 KO in TE13 cells markedly upregulated MET mRNA and c-MET protein levels (Figure 5A-D), suggesting that *MET* was the direct target gene of miR-198. High circLPAR3 expression remarkably increased the c-MET protein expression (Figure 5E), whereas low circLPAR3 expression dramatically decreased c-MET protein level, as well as the phosphorylation levels of its downstream proteins MAPK and AKT (Figure 5F). Transwell assay indicated that overexpression of miR-198 reversed the promoting effect of high circLPAR3 expression on ESCC cell migration (Figure 5G). Western blotting results indicated that overexpression of miR-198 reversed the upregulation of high circLPAR3 expression on c-MET level as well as the phosphorylation levels of its downstream proteins MAPK and AKT (Figure 5H). The above experimental results showed that circLPAR3 adsorbed miR-198 to upregulate MET expression and promote ESCC cell migration.

3.6 | CircLPAR3 promoted ESCC lung metastasis

The abovementioned experiments were the in vitro models at cell level. To more potently verify the effect of circLPAR3 on ESCC

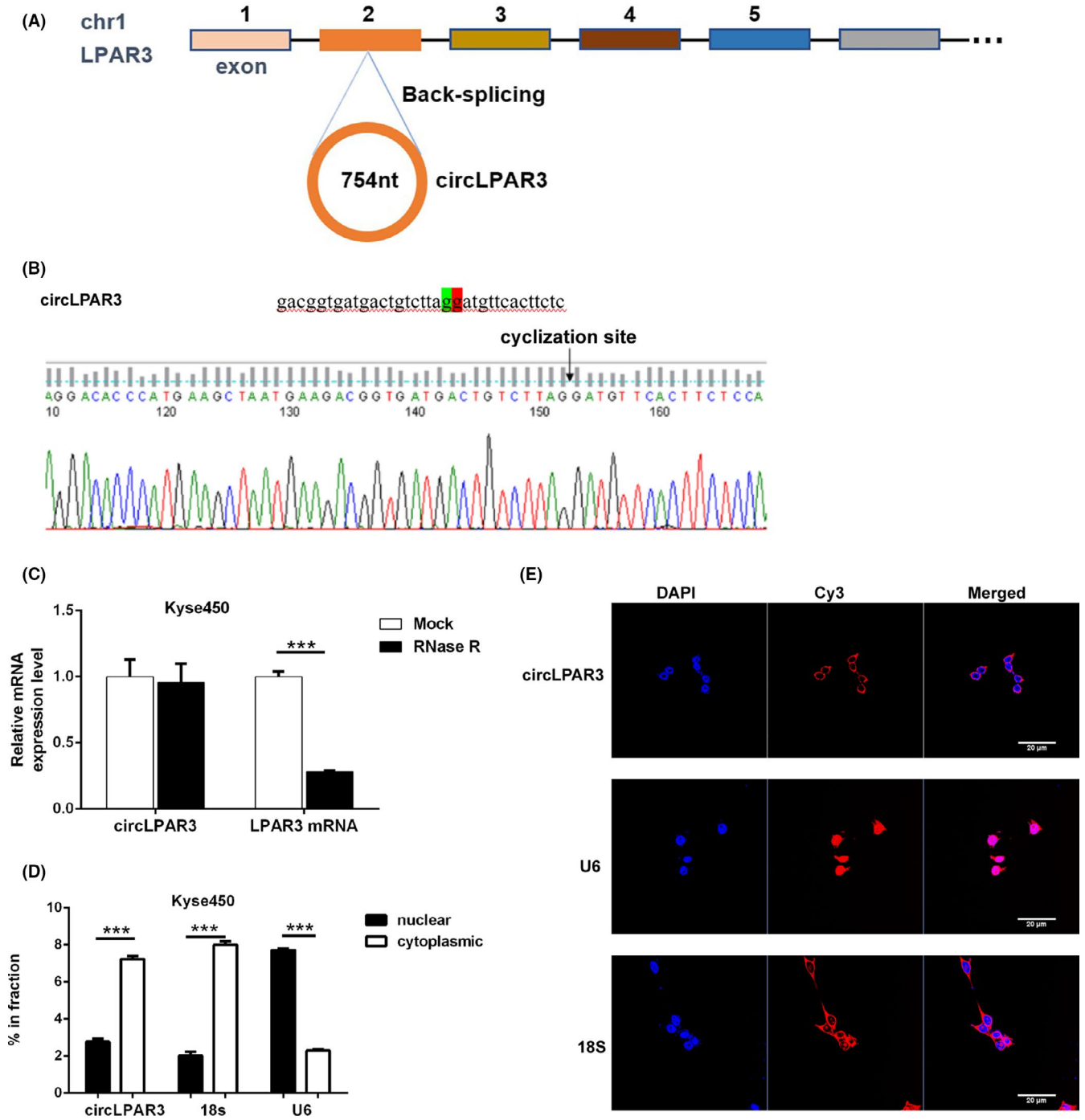

FIGURE 2 Biological characteristics of circular RNA LPAR3 (circLPAR3) in esophageal squamous cell carcinoma cells. A, CircLPAR3 origin, composition, and length. B, Sanger sequencing results of circLPAR3, in which the black arrow indicates the cyclization site. C, CircLPAR3 and linear LPAR3 mRNA expression in Kyse450 cells before and after RNase R treatment detected by quantitative RT-PCR. D, E, RNA nuclear-cytoplasmic separation (D) and FISH (E) experiments to understand circLPAR3 distribution in Kyse450 cells, with U6 and 18S rRNA as the positive controls of nuclear component and cytoplasmic component, respectively (scale bar = 20 μm). ***$P < .001$

metastasis and its molecular mechanism, we designed the in vivo model of passive ESCC metastasis. Transfection with sh-circLPAR#3 in TE13 cells markedly downregulated the circLPAR3 expression level (Figure 6A). TE13 cells with stably low circLPAR3 expression (shcircLPAR3#3) and control cells (shRNA control) were injected into 6-week-old nude mice through the caudal vein at the dose of 1×10^6 cells/100 μL. Mice were killed at 6 weeks after caudal vein injection, and the number of tumor nodules seen on the lung surface of the low circLPAR3 group was apparently less than those in the control group (Figure 6B). The H&E staining results of nude mouse lung tissue pathological sections indicated that the size and number of lung metastases in nude mice of low circLPAR3 group were apparently less than those in control group (Figure 6C,D). Additionally, IHC and qRT-PCR results suggested that the c-MET and MET expression in

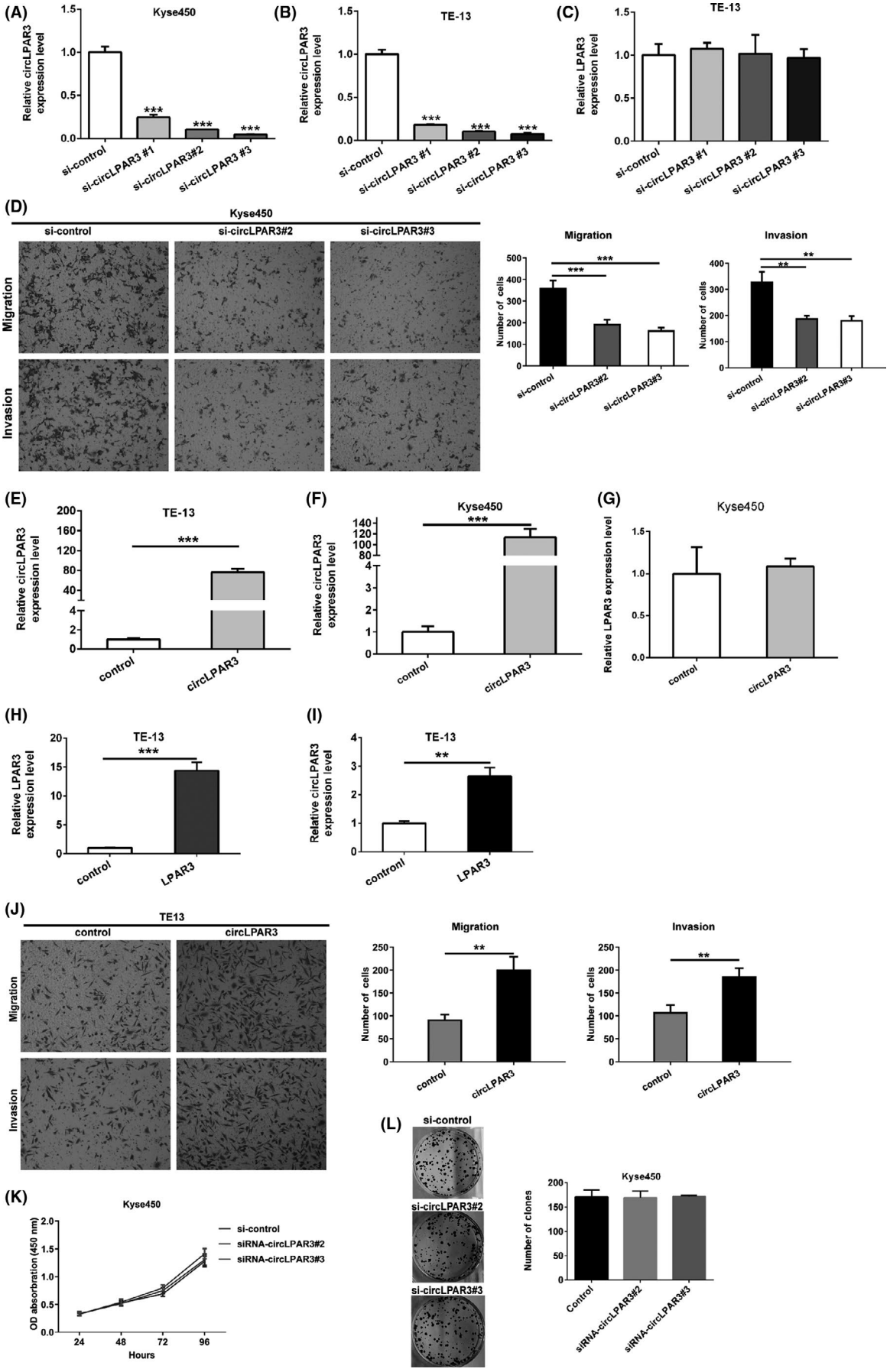
(A)
Kyse450
Relative circLPAR3 expression level
si-control
si-circLPAR3 #1
si-circLPAR3#2
si-circLPAR3 #3
(B)
TE-13
(C)
TE-13
Relative LPAR3 expression level
(D)
Kyse450
si-control
si-circLPAR3#2
si-circLPAR3#3
Migration
Invasion
Number of cells
(E)
TE-13
control
circLPAR3
(F)
Kyse450
(G)
Kyse450
(H)
TE-13
LPAR3
(I)
TE-13
(J)
TE13
control
circLPAR3
(K)
Kyse450
si-control
siRNA-circLPAR3#2
siRNA-circLPAR3#3
OD absorbration (450 nm)
Hours
(L)
si-control
si-circLPAR3#2
si-circLPAR3#3
Kyse450
Number of clones
Control
siRNA-circLPAR3#2
siRNA-circLPAR3#3

FIGURE 3 Circular RNA LPAR3 (circLPAR3) promotes esophageal squamous cell carcinoma cell migration and invasion in vitro. A, CircLPAR3 expression levels in si-circLPAR3-transfected Kyse450 cells detected by quantitative (q)RT-PCR. B, C, CircLPAR3 and LPAR3 expression levels in si-circLPAR3-transfected TE13 cells detected by qRT-PCR. D, Changes in Kyse450 cell migration and invasion capacities after downregulating circLPAR3 expression detected by Transwell assay. E, CircLPAR3 expression levels in TE13 cells transfected with high circLPAR3 expression plasmid detected by qRT-PCR. F, G, CircLPAR3 and LPAR3 expression levels in Kyse450 cells transfected with high circLPAR3 expression plasmid detected by qRT-PCR. H, I, Expression of LPAR3 and circLPAR3 in TE13 cells after LPAR3 overexpression plasmid transfection was determined by qRT-PCR. J, Effect of high circLPAR3 expression on TE13 cell migration and invasion capacities detected by Transwell assay. K, Proliferation of Kyse450 cells after circLPAR3 knockout for 24, 48, 72, and 96 h detected by CCK-8 assay. L, Kyse450 cell proliferation after circLPAR3 KO detected in cell colony formation assay. $^{**}P < .01$, $^{***}P < .001$

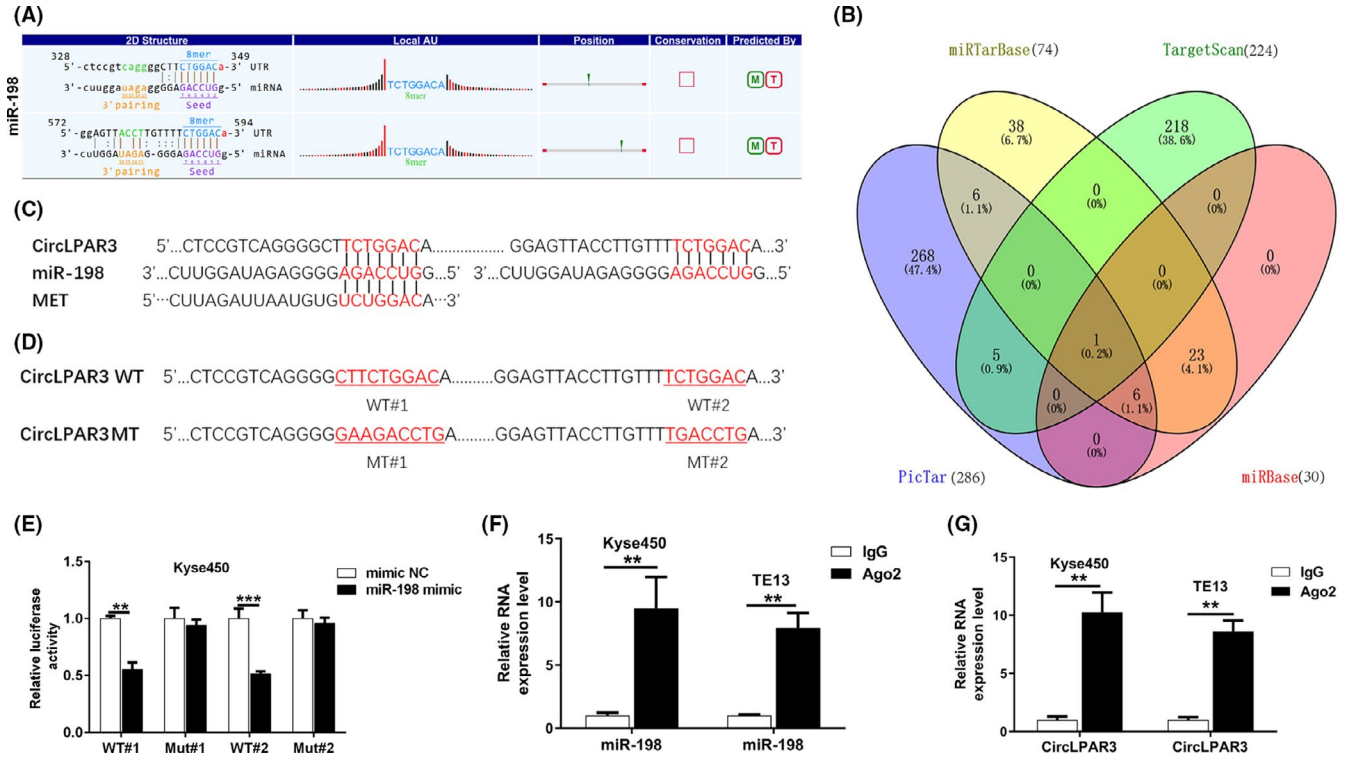

FIGURE 4 Circular RNA LPAR3 (circLPAR3) serves as a sponge of microRNA (miR)-198. A, Schematic diagram predicting the potential binding sites of circLPAR3 with miR-198. B, Venn diagram suggests the common downstream target genes of miR-198 predicted in 4 databases (PicTar, miRTarBase, TargetScan, and miRBase). C, Schematic diagram presenting the binding sites of circLPAR3-miR-198-MET. D, Dual-luciferase reporter gene plasmid mutation sites of circLPAR3. E, Luciferase activities detected after cotransfection of WT circLPAR3 or mutant circLPAR3 with miR-198 mimics or miR-198 mimic-negative control (NC) detected through dual-luciferase reporter gene assay. F, G, Binding of circLPAR3 and miR-198 with AGO2 protein in Kyse450 and TE13 cells detected through RIP assay. $^{**}P < .01$, $^{***}P < .001$

lung metastases of nude mice with low circLPAR3 expression was also apparently lower than that in control group (Figure 6E,F).

4 | DISCUSSION

In recent years, circRNAs have become the disease-related research hotspot second to miRNA and long noncoding RNA. More and more studies are carried out to examine the roles of circRNAs in tumor, including EC.[17] However, few studies focus on the expression and function of circRNAs in EC. In this study, high throughput sequencing was applied to screen the differentially expressed circRNAs in the 10 pairs of EC samples, and a novel circRNA (circLPAR3) with markedly elevated expression in tumor tissues was identified.

We discovered that circLPAR3 expression in EC tissues was apparently higher than that in paracarcinoma tissues, which was closely correlated with the pathological grade and LNM of EC patients. However, circLPAR3 expression was not obviously correlated with tumor infiltration depth, which might be related to the small number of ESCC patients in this study. We further confirmed that the expression of circLPAR3 were increased in ESCC cells. The LPAR3 overexpression plasmid could not only successfully increase the expression of linear LPAR3, but also increase circLPAR3 expression in ESCC cells, indicating that the elevated expression of circLPAR3 in ESCC tissues and cells was probably due to the increased expression of linear LPAR3. Moreover, in vitro and in vivo studies suggested that circLPAR3 promoted ESCC cell migration, invasion, and metastasis, but did not affect cell proliferation. Mechanically, circLPAR3 served as a sponge of miR-198 to upregulate the MET

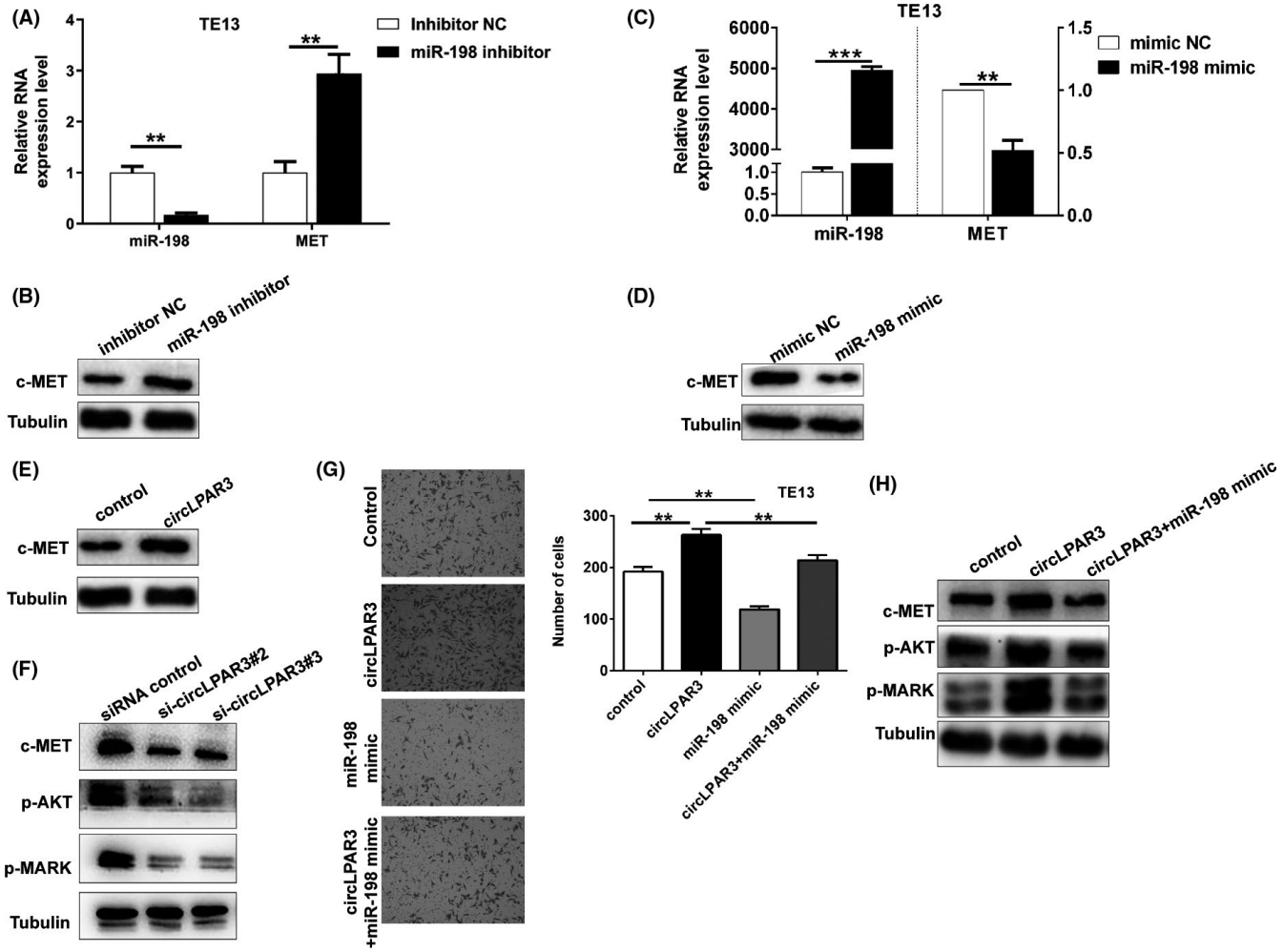

FIGURE 5 Circular RNA LPAR3 (circLPAR3) adsorbs microRNA (miR)-198 and targets MET to promote esophageal squamous cell carcinoma (ESCC) cell migration. A-D, Effects of downregulating and upregulating miR-198 expression on the *MET* gene and c-MET protein detected through quantitative RT-PCR and western blotting. E, Regulation of high circLPAR3 expression on c-MET protein level detected through western blotting. F, Regulation of low circLPAR3 expression on c-MET protein level and the phosphorylation levels of its downstream regulated proteins detected through western blotting. G, Transwell assay shows that overexpression of miR-198 can reverse the promoting effect of high circLPAR3 expression on ESCC cell migration. H, Regulation of miR-198 overexpression on the c-MET protein level and the phosphorylation levels of its downstream regulated proteins induced from the high circLPAR3 expression, as detected through western blotting. $^{*}P < .05$, $^{**}P < .01$, $^{***}P < .001$

expression level, thus promoting EC cell metastasis. To the best of our knowledge, this study is the first to report the role of circLPAR3 in ESCC.

Circular RNA is more stable than linear RNA, besides, it is enriched in cells, plasma, and even the circulatory exosome. Therefore, it can serve as the tumor diagnostic and therapeutic biomarker.[18,19] In our experiment, RNase R was adopted for cell treatment, which verified that circLPAR3 was more stable than the linear gene *LPAR3*. Combined with the previous study conclusions, high circLPAR3 expression is a high-risk factor of EC metastasis, but it remains to be further explored and investigated whether circLPAR3 detected in blood can serve as a biomarker of EC metastasis and prognosis.

Circular RNAs can be classified as exon circRNAs, intron circRNAs, exon-intron circRNAs (EIci RNAs) and intergenic circRNAs.[20] Of them, exon circRNAs are mainly located in cytoplasm, which are the richest circRNAs in the body.[21] Recent studies suggest that circRNA molecules are rich in miRNA response elements, which can competitively bind to miRNA, play a role as a miRNA sponge in cells, relieve the suppression of miRNA on its target gene, and upregulate the expression of target genes.[15,22] In this study, FISH and nuclear-cytoplasmic separation experiments verified that circLPAR3 was mainly located in the cytoplasm, which was able to regulate miRNAs at the posttranscription level. Circular RNA LPAR3 was verified in this study to serve as a sponge of miR-198 through bioinformatic analysis prediction, RIP, and luciferase assay.

MicroRNA-198 can regulate cell proliferation, migration, invasion, and apoptosis in pancreatic cancer and colon cancer, thus suppressing tumor development.[23-27] Tan et al verified that miR-198 was able to bind with and negatively regulate c-MET.[28] c-MET kinase is a type of transmembrane receptor with automatic phosphorylation activity encoded by the oncogene *MET*, which is

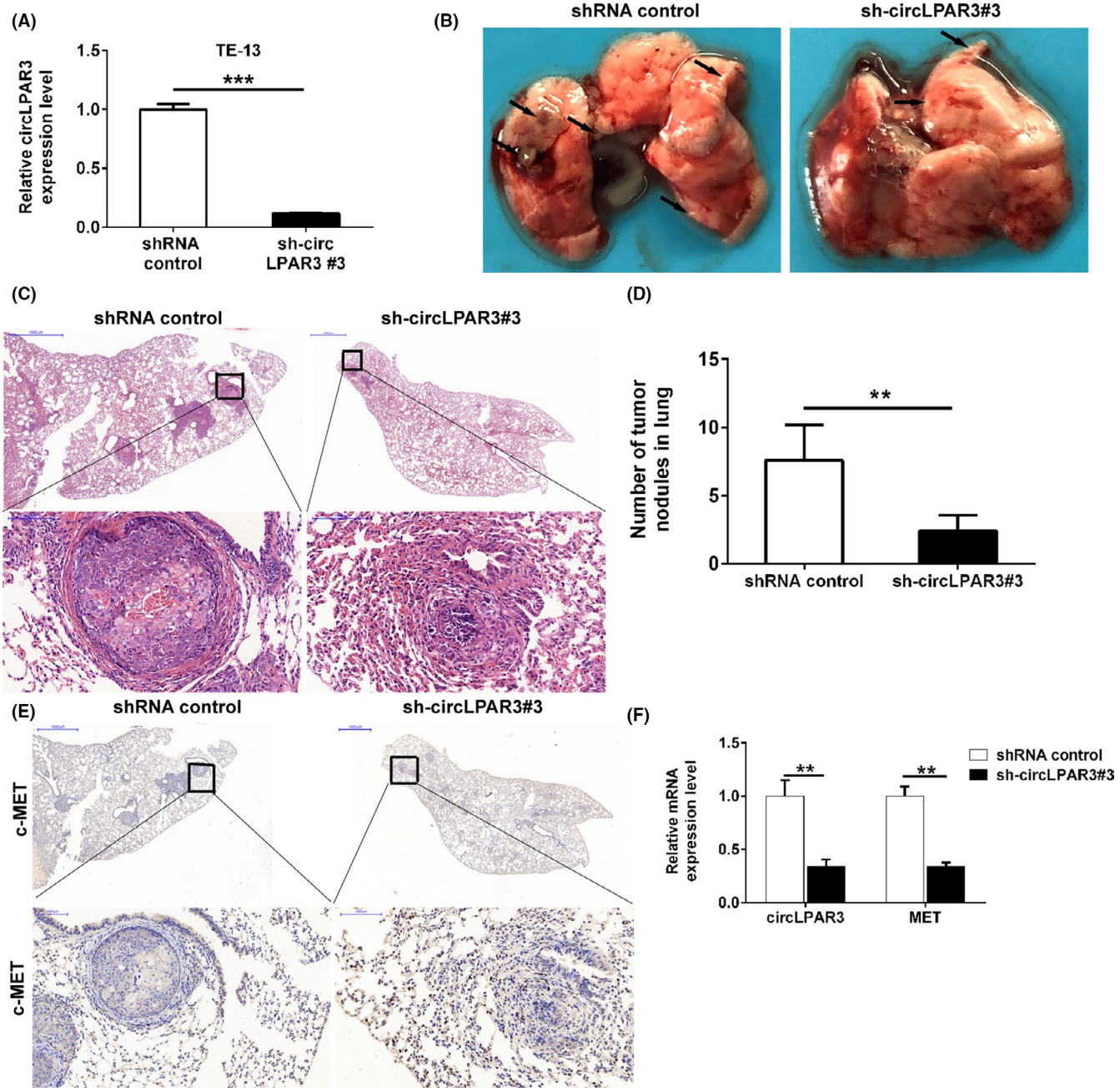

FIGURE 6 Circular RNA LPAR3 (circLPAR3) promotes esophageal squamous cell carcinoma lung metastasis in vivo. A, CircLPAR3 expression levels in sh-circLPAR3-transfected TE13 cells detected by quantitative (q)RT-PCR. B, Representative images of the tumor nodules could be seen on the lung surface in 2 groups of mice 6 wk after the tail vein injection of TE13 cells. C, Representative images of the H&E staining results of lung metastasis pathological sections in both groups (scale bars: upper, 1000 μm; lower, 100 μm). D, Quantitative analysis on the number of lung metastases in mice of both groups. E, Representative images of immunohistochemical results of lung metastases in both groups (scale bars: upper, 1000 μm; lower, 100 μm). F, Changes in circLPAR3 and MET expression in lung metastases of both groups detected through qRT-PCR. ***$P < .001$

expressed in both normal cells and tumor cells.[29] The persistent activation of c-MET is an important cause of tissue and cell carcinogenesis or enhanced cancer cell proliferation. c-MET is subjected to self-phosphorylation after it is activated, which can thereby activate the signaling pathways such as RAS/MAPK, PI3K/Akt, and STAT3/JNK, thus promoting tumor cell survival, proliferation, invasion, and angiogenesis.[30-32] This study verified the mechanism of circLPAR3 in regulating c-MET expression, which was that circLPAR3 adsorbed miR-198 as a sponge to weaken its suppression on c-MET expression, increase the phosphorylation of Akt and MAPK, affect the RAS/MAPK and PI3K/Akt pathways, and thus boost ESCC cell invasion and migration. We discovered in in vivo experiments that circLPAR3 KO downregulated MET expression and suppressed the lung metastasis of ESCC cells. Our study sufficiently showed that the circLPAR3-miR-198-MET signal axis played a vital regulatory role in ESCC (Figure 7).

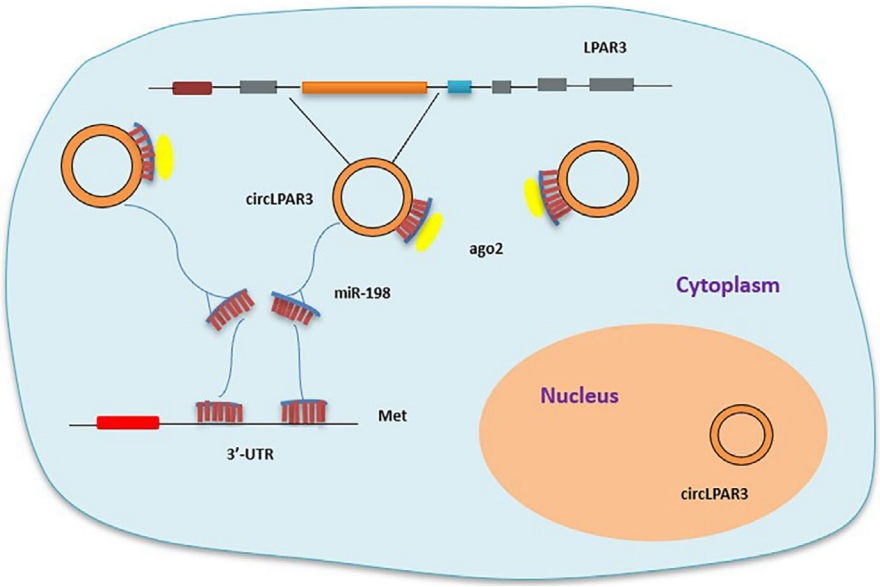

FIGURE 7 Schematic diagram of the circular RNA LPAR3 (circLPAR3)-microRNA (miR)-198-MET regulatory signal axis

To sum up, the circLPAR3 expression levels in ESCC tissues and cell lines are upregulated. In ESCC, high circLPAR3 expression is positively correlated with LNM and advanced tumor TNM stage. In vivo experiment proves that low circLPAR3 expression results in a lower risk of distant metastasis. CircLPAR3 serves as a sponge of miR-198 to regulate MET expression, thus promoting ESCC cell migration, invasion, and metastasis. The above findings support that circLPAR3 could serve as a diagnostic biomarker and therapeutic target of ESCC.

ACKNOWLEDGMENTS

We are grateful to Professor Jianwei Zhou and his team at the School of Public Health of Nanjing Medical University for their help in this research. This work was funded by the National Natural Science Foundation of China (project approval number: 81572263).

CONFLICT OF INTEREST

Authors declare no conflicts of interest for this article.

ORCID

Na Fang https://orcid.org/0000-0002-9628-0208
Yijiang Chen https://orcid.org/0000-0002-2434-5455

REFERENCES

1. Pennathur A, Gibson MK, Jobe BA, Luketich JD. Oesophageal carcinoma. *Lancet*. 2013;381:400-412.
2. Allemani C, Matsuda T, Di Carlo V, et al. Global surveillance of trends in cancer survival 2000–14 (CONCORD-3): analysis of individual records for 37 513 025 patients diagnosed with one of 18 cancers from 322 population-based registries in 71 countries. *Lancet*. 2018;391:1023-1075.
3. Headrick JR, Nichols FC, Miller DL, et al. High-grade esophageal dysplasia: long-term survival and quality of life after esophagectomy. *Ann Thorac Surg*. 2002;73:1697-1703.
4. Ohashi S, Miyamoto S, Kikuchi O, et al. Recent advances from basic and clinical studies of esophageal squamous cell carcinoma. *Gastroenterology*. 2015;149:1700-1715.
5. Guo JU, Agarwal V, Guo H, Bartel DP. Expanded identification and characterization of mammalian circular RNAs. *Genome Biol*. 2014;15:409.
6. Barrett SP, Wang PL, Salzman J. Circular RNA biogenesis can proceed through an exon-containing lariat precursor. *eLife*. 2015;4:e07540.
7. Barrett SP, Salzman J. Circular RNAs: analysis, expression and potential functions. *Development*. 2016;143:1838-1847.
8. Jeck WR, Sorrentino JA, Wang K, et al. Circular RNAs are abundant, conserved, and associated with ALU repeats. *RNA*. 2013;19:141-157.
9. Salzman J, Gawad C, Wang PL, Lacayo N, Brown PO. Circular RNAs are the predominant transcript isoform from hundreds of human genes in diverse cell types. *PLoS One*. 2012;7:e30733.
10. Wang PL, Bao Y, Yee M-C, et al. Circular RNA is expressed across the eukaryotic tree of life. *PLoS One*. 2014;9:e90859.
11. Qu S, Zhong Y, Shang R, et al. The emerging landscape of circular RNA in life processes. *RNA Biol*. 2017;14:992-999.
12. Chen Y, Li C, Tan C, Liu X. Circular RNAs: a new frontier in the study of human diseases. *J Med Genet*. 2016;53:359-365.
13. Ebert MS, Neilson JR, Sharp PA. MicroRNA sponges: competitive inhibitors of small RNAs in mammalian cells. *Nat Methods*. 2007;4:721-726.
14. Franco-Zorrilla JM, Valli A, Todesco M, et al. Target mimicry provides a new mechanism for regulation of microRNA activity. *Nat Genet*. 2007;39:1033-1037.
15. Poliseno L, Salmena L, Zhang J, et al. A coding-independent function of gene and pseudogene mRNAs regulates tumour biology. *Nature*. 2010;465:1033-1038.
16. Son H, Xu D, Shi PY, et al. Upregulated circRNA hsa_circ_0000337 promotes cell proliferation, migration, and invasion of esophageal squamous cell carcinoma. *Cancer Manage Res*. 2019;11:1997-2006.
17. Fan LY, Cao Q, Liu J, Zhang JP, Li BS. Circular RNA profiling and its potential for esophageal squamous cell cancer diagnosis and prognosis. *Mol Cancer*. 2019;18:16.
18. Chen B, Huang S. Circular RNA: an emerging non-coding RNA as a regulator and biomarker in cancer. *Cancer Lett*. 2018;418:41-50.
19. Li Y, Zheng Q, Bao C, et al. Circular RNA is enriched and stable in exosomes: a promising biomarker for cancer diagnosis. *Cell Res*. 2015;25:981-984.

20. Wang FL, Nazarali AJ, Ji SP. Circular RNAs as potential biomarkers for cancer diagnosis and therapy. *Am J Cancer Res*. 2016;6:1167-1176.
21. Li Z, Huang C, Bao C, et al. Exon-intron circular RNAs regulate transcription in the nucleus. *Nat Struct Mol Biol*. 2015;22:256-264.
22. Cesana M, Cacchiarelli D, Legnini I, et al. A long noncoding RNA controls muscle differentiation by functioning as a competing endogenous RNA. *Cell*. 2011;147:358-369.
23. Marin-Muller C, Li D, Bharadwaj U, et al. A tumorigenic factor interactome connected through tumor suppressor microRNA-198 in human pancreatic cancer. *Clin Cancer Res*. 2013;19:5901-5913.
24. Wang M, Wang J, Kong X, et al. MiR-198 represses tumor growth and metastasis in colorectal cancer by targeting fucosyl transferase 8. *Sci Rep*. 2014;4:6145.
25. Yip L, Kelly L, Shuai Y, et al. MicroRNA signature distinguishes the degree of aggressiveness of papillary thyroid carcinoma. *Ann Surg Oncol*. 2011;18:2035-2041.
26. Ray J, Hoey C, Huang X, et al. MicroRNA-198 suppresses prostate tumorigenesis by targeting MIB1. *Oncol Rep*. 2019;42:1047-1056.
27. Yang J, Zhao H, Xin Y, Fan LM. MicroRNA-198 inhibits proliferation and induces apoptosis of lung cancer cells via targeting FGFR1. *J Cell Biochem*. 2014;11:987-995.
28. Tan S, Li R, Ding K, Lobie PE, Zhu T. miR-198 inhibits migration and invasion of hepatocellular carcinoma cells by targeting the HGF/c-MET pathway. *FEBS Lett*. 2011;585:2229-2234.
29. Hanna JA, Bordeaux J, Rimm DL, Agarwal S. The function, proteolytic processing, and histopathology of Met in cancer. *Adv Cancer Res*. 2009;103:1-23.
30. Kim KJ, Wang LH, Su YC, et al. Systemic anti-hepatocyte growth factor monoclonal antibody therapy induces the regression of intracranial glioma xenografts. *Clin Cancer Res*. 2006;12:1292-1298.
31. Blumenschein GR, Mills GB, Gonzalez-Angulo AM. Targeting the hepatocyte growth factor-cMET axis in cancer therapy. *J Clin Oncol*. 2012;30:3287-3296.
32. Zhang YW, Su Y, Volpert OV, Woude GFV. Hepatocyte growth factor/scatter factor mediates angiogenesis through positive VEGF and negative thrombospondin 1 regulation. *Proc Natl Acad Sci*. 2003;100:12718-12723.

How to cite this article: Shi Y, Fang N, Li Y, et al. Circular RNA LPAR3 sponges microRNA-198 to facilitate esophageal cancer migration, invasion, and metastasis. *Cancer Sci*. 2020;111:2824–2836. https://doi.org/10.1111/cas.14511